Tetrahedron Letters 50 (2009) 4430–4434

Contents lists available at ScienceDirect

Tetrahedron Letters

journal homepage: www.elsevier.com/locate/tetlet

Controlled self-assembly of chiral gelator molecules into aligned fibers induced by nematic to smectic B phase transitions

Nataša Šijaković Vujičić [a], Maja Šepelj [b], Andreja Lesac [b], Mladen Žinić [a,*]

[a] Laboratory of Supramolecular and Nucleoside Chemistry, Rudjer Boskovic Institute, Bijenicka 54, Zagreb 10000, Croatia
[b] Laboratory for Stereoselective Catalysis and Biocatalysis, Rudjer Boskovic Institute, Bijenicka 54, Zagreb 10000, Croatia

ARTICLE INFO

Article history:
Received 8 April 2009
Revised 30 April 2009
Accepted 15 May 2009
Available online 23 May 2009

Keywords:
Self-assembly
Gelator
Liquid crystalline gel
Aligned fibers
Controlled self-assembly

ABSTRACT

Chiral bisoxalamide **1** shows remarkable gelling capacity of the nematic and smectic B liquid-crystalline phases of heptylcyclohexanecarboxylic acid (**HCCA**). Chiral nematic-containing left-handed helical fiber bundles are formed if the gelator is present in amounts higher than 0.55 wt %. With lower amounts of **1**, no nematic gel forms, however, a nematic to smectic B phase transition triggers instantaneous self-assembly of gelator molecules into aligned fibers. The latter liquid crystalline gel system represents an example of controlled self-assembly induced by a liquid crystalline phase transition.

Research has shown that a small quantity of low molecular weight organic gelators can gel large volumes of various organic solvents or water, efficiently, giving organogels and hydrogels, respectively.[1] In addition, the group of Kato has reported on the formation of liquid crystalline gels (LC gels) where a liquid crystalline phase was gelled playing the role of an ordinary solvent.[2] The latter systems represent a new type of soft materials which may possess induced or enhanced electro-optical,[3] photochemical,[4] and electronic[5] properties which are useful for the construction of supramolecular devices for advanced applications. LC gels represent more complex systems consisting of a mesogen and a gelator each capable of giving different types of supramolecular organization at a specific temperature. Usually, the LC gels exhibit random or ordered phase-separated structures depending on the relation between sol–gel ($T_{sol-gel}$) and isotropic-LC (T_{iso-lc}) transition temperatures. When $T_{sol-gel}$ is higher than T_{iso-lc} (Type I), a randomly dispersed network of gelator fibers is formed in the isotropic state of the liquid crystal.[6] In contrast, when T_{iso-lc} is higher than $T_{sol-gel}$ (Type II), the anisotropic LC media serves as a template for anisotropic growth of gel fibers.[7,3a] Until now, LC gels of nematic, smectic A and C, and discotic columnar phases have been reported which in some cases formed at a gelator concentration as low as 0.25 wt %. However, the behavior of gelator molecules in an organized smectic B phase and its unexpected influence on the self-assembly of gelator molecules resulting in formation of highly aligned fibers have not been reported to date.

Here, we report on the gelation of nematic and smectic B LC phases formed by mesogen heptylcyclohexanecarboxylic acid (**HCCA**) and provide evidence that gelation of each phase depends substantially on the concentration of chiral gelator **1**. When **1** is present in concentrations higher than 0.55 wt % it induces initially the transformation of the nematic phase into a chiral nematic (cholesteric) phase which upon further cooling is gelled by **1**. In contrast, with **1** present in the concentration range 0.025–0.5 wt %, neither chiral induction nor gelation of the nematic phase was observed. However, the subsequent transition, at lower temperatures, of the nematic phase containing **1** into a homeotropically oriented smectic B phase triggers instantaneous self-assembly of the gelator molecules into aligned fibrous aggregates. We provide differential scanning calorimetry (DSC), FTIR, and electron microscopic evidence that the LC phase transition from nematic to organized and viscous smectic B phase is able to trigger instantaneously the self-assembly of gelator molecules into fibrous aggregates and also serves as a template for their alignment.

In continuation of our studies on oxalamide gelators,[8] a new type of chiral bisoxalamide gelator has been designed and their gelation ability and sol–gel transcription into various silica fibers examined[9] (Scheme 1). We also found that chiral gelator **1** shows remarkable gelation capacity for the liquid crystalline (LC) phases of **HCCA**. It is known that **HCCA** displays two mesophases, nematic and smectic B.[10]

Addition of various amounts of gelator **1** resulted in the formation of type II LC gels ($T_{iso-lc} > T_{sol-gel}$). When **1** was used in the concentration range 0.55–5.5 wt %, the mixture, upon cooling from an isotropic liquid displays a chiral (cholesteric) nematic phase

* Corresponding author. Tel.: +385 1 456 1061; fax: +385 1 468 0195.
E-mail address: zinic@irb.hr (M. Žinić).

0040-4039/$ - see front matter © 2009 Elsevier Ltd. All rights reserved.
doi:10.1016/j.tetlet.2009.05.058

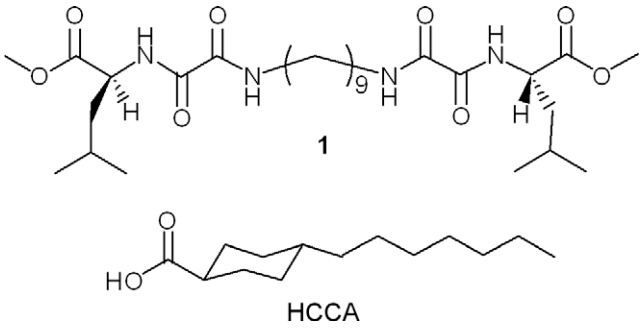

Scheme 1. Structures of bisoxalamide gelator **1** and mesogen **HCCA**.

characterized by the typical fingerprint texture shown in Figure 1a (polarizing optical microscope; cooling rate 5 °C min^{-1}).

Formation of the chiral LC phase can be explained by the presence of chiral dopand **1** initially dissolved in the isotropic state of **HCCA**. By further cooling of the cholesteric phase it hardens due to gelation by **1**. As the polarizing optical photomicrograph shows, the fingerprint texture remains in the newly formed LC gel (Fig. 1b). However, when **1** is present in a lower concentration range (0.025–0.5 wt %) no chiral induction was observed. Monitoring of the cooling process throughout the latter concentration regime using a polarizing optical microscope shows initial formation of a nematic phase (Fig. 1c), however, formation of a gel was not observed in this case. Further cooling of the sample results in the formation of the homeotropically oriented smectic B phase; Figure 1d shows initial transition of nematic to the homeotropically oriented smectic B phase appearing as dark regions in the micrograph. Upon further cooling, the optical micrographs show the formation of a gel network consisting of thick gel fibers with diameters of 1–2 μm (Fig. 1e and f); several domains containing aligned fibers can be clearly seen in the micrographs. It should be noted that the formation of fibrous aggregates in the smectic B phase can be observed even in the presence of only 0.025 wt % of **1** (Fig. 2).

Besides polarizing optical microscopy, the LC and sol-to-gel phase transitions were monitored by DSC calorimetry. Measurements performed with a cooling rate of 5 °C min^{-1} gave only broad overlapped peaks for nematic to smectic B and sol-to-gel transitions. However, at a cooling rate of 2 °C min^{-1}, well-separated peaks for LC and sol-to-gel transitions were obtained (Fig. 2).

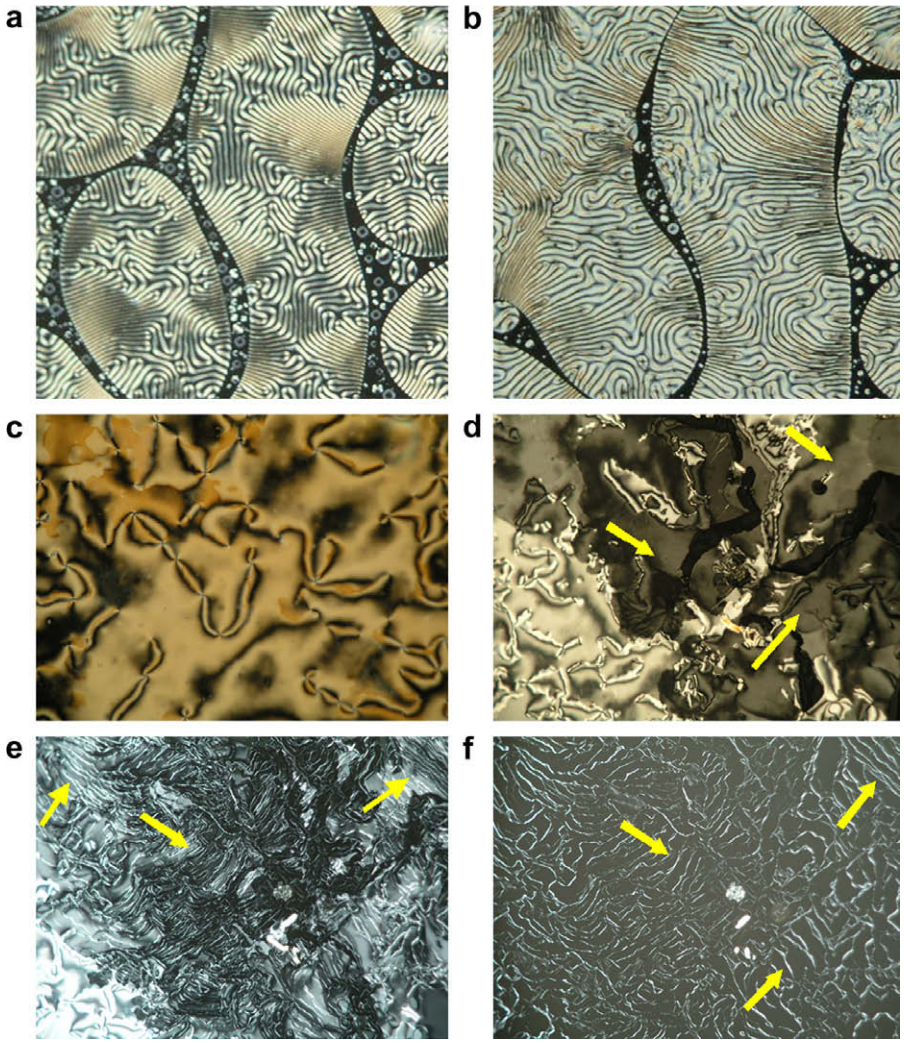

Figure 1. Polarizing optical photomicrographs for the mixture containing 3 wt % of **1** in **HCCA**, showing (a) the fingerprint texture of the chiral nematic phase observed at 99 °C, and (b) the chiral nematic gel state at 81 °C, and for the mixture containing 0.3 wt % of **1** in **HCCA** showing (c) a nematic phase at 93 °C, (d) initial transition of the nematic to a homeotropically oriented smectic B phase at 77.8 °C visible by the appearance of dark regions (arrows), (e) domains of aligned fibers (arrows) formed within the homeotropically oriented smectic B phase at 77.5 °C, and (f) fibrous aggregates and domains of aligned fibers (arrows) in fully homeotropically organized smectic B phase at 76.5 °C. No rubbed surfaces were used in these experiments.

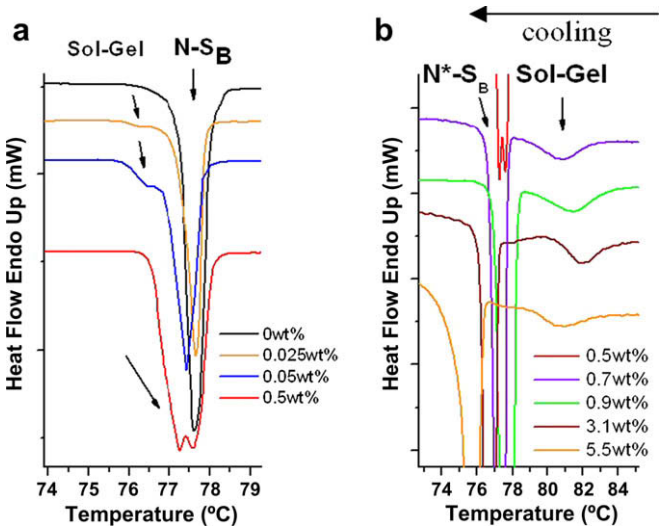

Figure 2. DSC cooling curves (cooling rate, 2 °C min^{-1}) for **1/HCCA** mixtures: (a) 0.025–0.5 wt % of **1** (smectic B gels), and (b) 0.7–5.5 wt % of **1** (chiral nematic gels).

DSC measurements of **1/HCCA** mixtures with **1** present in the lower concentration regime (0.025–0.5 wt %) showed one strong peak corresponding to a nematic to smectic B transition and a shoulder at slightly lower temperatures due to the sol-to-gel transition (Fig. 2a). Clearly, the DSC results prove that at low concentrations of **1**, the transition of the nematic into a smectic B phase precedes the sol-to-gel transition. On the other hand, at concentrations of **1** in the range of 0.55–5.5 wt %, DSC shows broad peaks at higher temperatures corresponding to the sol-to-gel transition within the chiral nematic phase followed by a strong peak for the chiral nematic to smectic B transition (Fig. 2b). The phase diagram constructed on the basis of DSC measurements in the cooling regime for various **1/HCCA** mixtures is shown in Figure 3. It should be emphasized that for all the reported examples of LC gels, the sol-to-gel transition curves were hyperbolic in shape for the entire range of gelator concentrations independently of the LC phase transitions.[5,7]

However, the phase diagram in Figure 3 clearly shows two distinctly different sol-to-gel transition curves for chiral nematic and smectic B phases at higher and lower concentration ranges of **1**.

It should be noted that the sol-to-gel transition in the smectic B phase occurs at considerably higher temperatures than those that would appear by extrapolation of the hyperbolic chiral nematic curve into the smectic B region, which also contrasts the results reported until now. Apparently, the self-assembly of gelator molecules is forced to occur at higher temperatures in the much more organized and more viscous smectic B phase compared to the less organized and more fluid nematic phase.

The phase diagram of the heating regime constructed from DSC measurements of different **1/HCCA** mixtures shows the hyperbolic shape of the gel-to-sol transition curve (Fig. 4) in contrast to that obtained for the cooling regime.

The transition temperature of the smectic B phase-containing gel network to nematic gel state is lower than the gel-to-sol transition temperature for the entire concentration range of **1**. The gel-to-sol transition in the entire concentration range occurs within the nematic and isotropic phases and gives a hyperbolic curve. In contrast to the cooling cycle, here the LC phase transition has no effect on the gel-to-sol transition.

To identify intermolecular interactions that stabilize gelator assemblies in liquid crystalline gels the corresponding FTIR spectra were analyzed. At room temperature, the NH band appears at

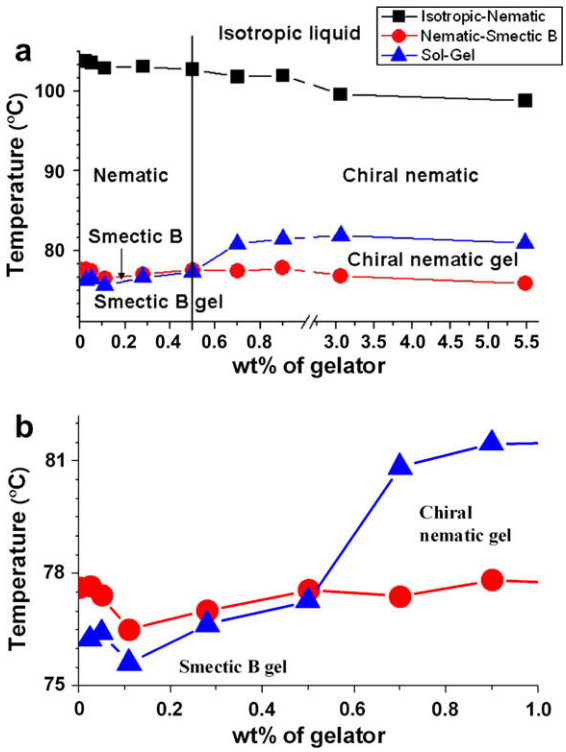

Figure 3. (a) Phase diagram for the cooling cycle for various compositions of **1/HCCA** mixtures constructed by DSC measurements (cooling rate 2 °C min^{-1}); (b) enlarged region of the diagram for the concentrations of **1** between 0.025 and 1.0 wt%.

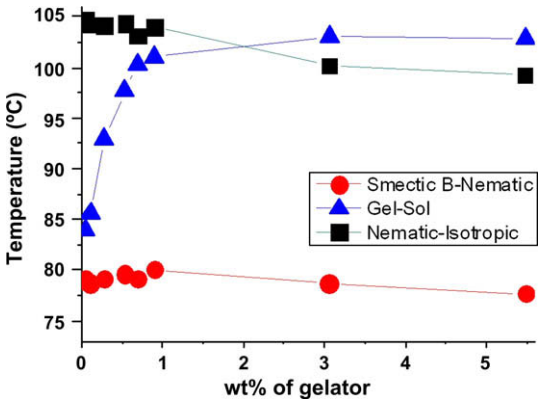

Figure 4. Phase diagram for the heating cycle of **1/HCCA** mixtures.

3293 cm^{-1}, the amide I at 1654 cm^{-1}, and the amide II at 1522 cm^{-1} corresponding to the hydrogen-bonded NH and C=O functionalities of the oxalamide units. In the spectra of the isotropic solution of gelator **1** in the mesogen **HCCA** at 110 °C, the NH, amide I, and amide II bands were shifted to higher wavenumbers (NH 3397 cm^{-1}, amide I is overlapped with the CO(OH) band of the LC compound at 1700 cm^{-1} and amide II is at 1506 cm^{-1}) indicating disassembly and disruption of the intermolecular hydrogen bonds between oxalamide units. The LC gel-to-sol transitions are thermoreversible and could be followed by the observed shifts of the FTIR bands.

SEM images of the remaining fiber network after washing out the **HCCA** (hexane) in the chiral nematic gel (3.0 wt % of **1**; Fig. 5a), and the smectic B gel (0.1 wt % of **1**; Fig. 5b), reveal distinctly different morphologies characterized by the presence of

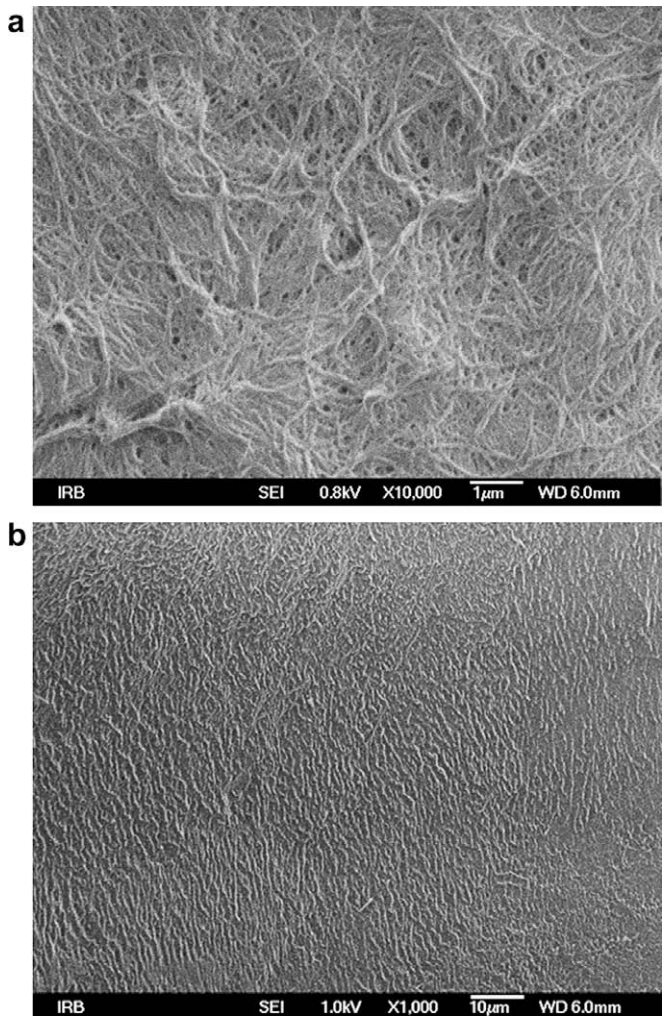

Figure 5. SEM images of **1**/**HCCA** LC gels obtained after washing out the **HCCA** with hexane: (a) gel network image of the chiral nematic gel containing 3 wt % of **1**; (b) gel network image of the smectic B gel containing 0.1 wt % of **1**.

long and heavily entangled fibers in the first system and much more oriented fibers in the second.

The TEM image of the chiral nematic gel shows that the network consists of helical left-handed fiber bundles with diameters of 40–100 nm (Fig. 6a) composed of much thinner fibers, with diameters of around 10 nm. In contrast, much shorter and highly aligned fibrous aggregates with diameters of 10–20 nm and lengths between 80 and 700 nm were observed in the smectic B gel (Fig. 6b; fibers of similar dimensions were also observed by atomic force microscopy (AFM); see Supplementary data). It should be emphasized that no oriented surfaces were used in these experiments.

In summary, the results show that using **HCCA** as the mesogen, which is capable of giving two different liquid crystalline phases (nematic and smectic B), and chiral gelator **1**, two distinctly different liquid crystalline gel systems are obtained, depending on the concentration of the gelator. The two LC gel systems differ in the morphology of the gel assemblies: (i) left-handed helical bundles are formed in the chiral nematic LC gel at concentrations of **1** higher than 0.55 wt %, and (ii) straight and highly aligned fibrous assemblies form in the smectic B phase at 0.025–0.5 wt % of **1**. At the higher concentration regime, the chiral nematic phase is gelled, which upon cooling, transforms into a smectic B gel retaining a typical gel network morphology consisting of heavily entangled fiber bundles. Once a gel network is formed in the chiral nematic phase, its transition to the smectic B phase does not affect the organization of gelator molecules.

In the lower concentration range of **1**, the nematic phase was not gelled, but aligned fibrous gelator aggregates formed instantaneously after the nematic-to-homeotropically oriented smectic B phase transition had occurred. In contrast to the less organized and more fluidic nematic phase, the self-assembly of gelator molecules within the much more organized and viscous smectic B phase occurred at concentrations of **1** at least 20 times lower (0.025 wt %) than those necessary for gelation of the chiral nematic mesophase (0.55 wt %). Apparently, the organized and viscous smectic B phase serves as a template triggering the self-assembly of gelator molecules into aligned fibrous aggregates. The results described herein may open new possibilities for the preparation of LC phase-controlled self-assembled systems and production of

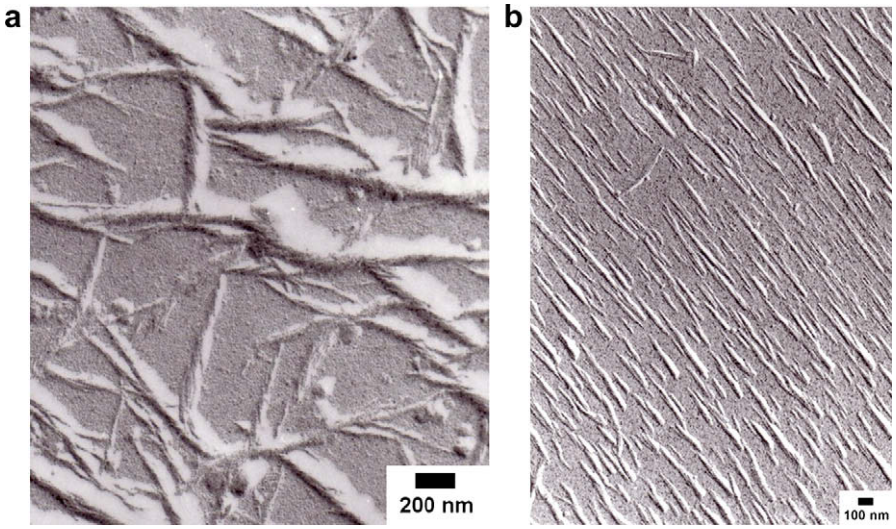

Figure 6. TEM images (Pd shadowing) of **1**/**HCCA** LC gels: (a) image of the chiral nematic gel showing left-handed helical bundles, (b) TEM image showing highly oriented fiber assemblies formed in the smectic B gel at 0.5 wt % of gelator **1**.

unidirectionally aligned assemblies. The latter may be of interest for production of nano-sized aligned functional assemblies with potential application in optoelectronic, photochemical, or catalytic nano-devices.

Acknowledgment

We gratefully acknowledge the financial support of the Croatian Ministry of Science and Technology (Project No. 098-0982904-2912).

Supplementary data

Supplementary data associated with this article can be found, in the online version, at doi:10.1016/j.tetlet.2009.05.058.

References and notes

1. (a) Liu, X. Y.; Žinić, M.; Vögtle, F.; Fages, F.; Araki, K.; Yoshikawa, I.; Brizard, A.; Oda, R.; Huc, I.; Kato, T.; Mizoshita, N.; Moriyama, M.; Kitamura, T.; Hirst, A. R.; Smith, D. K.. In *Low Molecular Mass Gelators. Design, Self-Assembly, Function*; Fages, F., Ed.; Springer: Berlin, 2005; Vol. 256, pp 1–283; (b) Sangeetha, N. M.; Maitra, U. *Chem. Soc. Rev.* **2005**, *34*, 821–836; (c) Terech, P.; Weiss, R. G. *Chem. Rev.* **1997**, *97*, 3133–3159; (d) Estroff, L. A.; Hamilton, A. D. *Chem. Rev.* **2004**, *104*, 1201–1217; (e) Gronwald, O.; Shinkai, S. *Chem. Eur. J.* **2001**, *7*, 4328–4334; (f) Ahmed, S. A.; Sallenave, X.; Fages, F.; Mieden-Gundert, G.; Muller, W. M.; Muller, U.; Vogtle, F.; Pozzo, J.-L. *Langmuir* **2002**, *18*, 7096–7101; (g) de Jong, J. J. D.; Lucas, L. N.; Kellogg, R. M.; van Esch, J. H.; Feringa, B. L. *Science* **2004**, *304*, 278–281; (h) Frkanec, L.; Jokic, M.; Makarevic, J.; Wolsperger, K.; Zinic, M. *J. Am. Chem. Soc.* **2002**, *124*, 9716–9719; (i) Hanabusa, K.; Tanaka, R.; Suzuki, M.; Kimura, M.; Shirai, H. *Adv. Mater.* **1997**, *9*, 1095–1097.
2. (a) Kato, T.; Hirai, Y.; Nakaso, S.; Moriyama, M. *Chem. Soc. Rev.* **2007**, *36*, 1857–1867; (b) Kato, T.; Mizoshita, N.; Kishimoto, K. *Angew. Chem., Int. Ed.* **2006**, *45*, 38–68; (c) Kato, T.; Mizoshita, N.; Moriyama, M.; Kitamura, T. *Top. Curr. Chem.* **2005**, *256*, 219–236; (d) Kato, T. *Science* **2002**, *295*, 2414–2418.
3. (a) Mizoshita, N.; Hanabusa, K.; Kato, T. *Adv. Funct. Mater.* **2003**, *13*, 313–317; (b) Tong, X.; Zhao, Y. *J. Mater. Chem.* **2003**, *13*, 1491–1495; (c) Tong, X.; Zhao, Y.; An, B. K.; Park, S. Y. *Adv. Funct. Mater.* **2006**, *16*, 1799–1804; (d) Tong, X.; Zhao, Y. *J. Am. Chem. Soc.* **2007**, *129*, 6372–6373; (e) Mizoshita, N.; Suzuki, Y.; Hanabusa, K.; Kato, T. *Adv. Mater.* **2005**, *17*, 692–696.
4. (a) Moriyama, M.; Mizoshita, N.; Yokota, T.; Kishimoto, K.; Kato, T. *Adv. Mater.* **2003**, *15*, 1335–1338; (b) Moriyama, M.; Mizoshita, N.; Kato, T. *Polym. J.* **2004**, *36*, 661–664; (c) Zhao, Y.; Tong, X. *Adv. Mater.* **2003**, *15*, 1431–1435; (d) Mizoshita, N.; Kato, T. *Adv. Funct. Mater.* **2006**, *16*, 2218–2224.
5. (a) Mizoshita, N.; Monobe, H.; Inoue, M.; Ukon, M.; Watanabe, T.; Shimizu, Y.; Hanabusa, K.; Kato, T. *Chem. Commun.* **2002**, 428–429; (b) Kitamura, T.; Nakaso, S.; Mizoshita, N.; Tochigi, Y.; Shimomura, T.; Moriyama, M.; Ito, K.; Kato, T. *J. Am. Chem. Soc.* **2005**, *127*, 14769–14775; (c) Yabuuchi, K.; Tochigi, Y.; Mizoshita, N.; Hanabusa, K.; Kato, T. *Tetrahedron* **2007**, *63*, 7358–7365.
6. (a) Kato, T.; Kutsuna, T.; Hanabusa, K.; Ukon, M. *Adv. Mater.* **1998**, *10*, 606–608; (b) Kato, T.; Kondo, G.; Hanabusa, K. *Chem. Lett.* **1998**, *27*, 193–195; (c) Guan, L.; Zhao, Y. *Chem. Mater.* **2000**, *12*, 3667–3673.
7. (a) Mizoshita, N.; Kutsuna, T.; Hanabusa, K.; Kato, T. *Chem. Commun.* **1999**, 781–782; (b) Guan, L.; Zhao, Y. *J. Mater. Chem.* **2001**, *11*, 1339–1344; (c) Kato, T.; Kutsuna, T.; Yabuuchi, K.; Mizoshita, N. *Langmuir* **2002**, *18*, 7086–7088; (d) Zhao, Y.; Guan, L. *Liq. Cryst.* **2003**, *30*, 81–86.
8. (a) Jokić, M.; Čaplar, V.; Portada, T.; Makarević, J.; Šijaković Vujičić, N.; Žinić, M. *Tetrahedron Lett.* **2009**, *50*, 509–513; (b) Fages, F.; Vögtle, F.; Žinić, M.. In *Low Molecular Mass Gelators. Design, Self-Assembly, Function*; Fages, F., Ed.; Springer: Berlin, 2005; Vol. 256, pp 77–131; (c) Makarević, J.; Jokić, M.; Perić, B.; Tomišić, V.; Kojić-Prodić, B.; Žinić, M. *Chem. Eur. J.* **2001**, *7*, 3328–3341; (d) Makarević, J.; Jokić, M.; Frkanec, L.; Katalenić, D.; Žinić, M. *Chem. Commun.* **2002**, 2238–2239; (e) Makarević, J.; Jokić, M.; Raza, Z.; Štefanić, Z.; Kojić-Prodić, B.; Žinić, M. *Chem. Eur. J.* **2003**, *9*, 5567–5580; (f) Džolić, Z.; Wolsperger, K.; Žinić, M. *New J. Chem.* **2006**, *30*, 1411–1419.
9. Šijaković-Vujičić, N.; Ljubešić, N.; Žinić, M. *Croat. Chem. Acta* **2007**, *80*, 591–598.
10. Phase transitions for **HCCA:** Cr_2 31 (13.46 kJ/mol) Cr_1 54 (5.20 kJ/mol) B 77 (2.43 kJ/mol) N 104 (1.25 kJ/mol): Billard, J.; Mamlok, L. *Mol. Cryst. Liq. Cryst.* **1978**, *41*, 217–222.